RESEARCH REPORT

PEG10 viral aspartic protease domain is essential for the maintenance of fetal capillary structure in the mouse placenta

Hirosuke Shiura[1,2], Ryuichi Ono[3], Saori Tachibana[2], Takashi Kohda[1,2], Tomoko Kaneko-Ishino[4,*] and Fumitoshi Ishino[2,*]

ABSTRACT

The therian-specific gene paternally expressed 10 (*Peg10*) plays an essential role in placenta formation: *Peg10* knockout mice exhibit early embryonic lethality as a result of severe placental defects. The PEG10 protein exhibits homology with long terminal repeat (LTR) retrotransposon GAG and POL proteins; therefore, we generated mice harboring a mutation in the highly conserved viral aspartic protease motif in the POL-like region of PEG10 because this motif is essential for the life cycle of LTR retrotransposons/retroviruses. Intriguingly, frequent perinatal lethality, not early embryonic lethality, was observed with fetal and placental growth retardation starting mid-gestation. In the mutant placentas, severe defects were observed in the fetal vasculature, where PEG10 is expressed in the three trophoblast cell layers that surround fetal capillary endothelial cells. Thus, *Peg10* has essential roles, not only in early placenta formation, but also in placental vasculature maintenance from mid- to late-gestation. This implies that along the feto-maternal placenta interface an interaction occurs between two retrovirus-derived genes, *Peg10* and retrotransposon Gag like 1 (*Rtl1*, also called *Peg11*), that is essential for the maintenance of fetal capillary endothelial cells.

KEY WORDS: **Peg10, Rtl1, Gene domestication (exaptation), Placenta development, Placental vascular dysfunction, Eutherian placenta evolution**

INTRODUCTION

PEG10 is a therian-specific gene encoding GAG- and POL-like proteins that exhibit at most ~20-30% homology with the long terminal repeat (LTR) sushi-ichi retrotransposon (Ono et al., 2001). Certain characteristic traits, such as the presence of a CCHC RNA-binding domain in the GAG-like region, a DSG viral aspartic protease motif in the POL-like region and a −1 ribosomal frameshift

[1]Faculty of Life and Environmental Sciences, University of Yamanashi, Yamanashi 400-8510, Japan. [2]Department of Epigenetics, Medical Research Institute (MRI), Tokyo Medical and Dental University (TMDU), Tokyo 113-8510, Japan. [3]Division of Cellular and Molecular Toxicology, Center for Biological Safety and Research, National Institute of Health Sciences (NIHS), Kanagawa 210-9501, Japan. [4]Faculty of Nursing, School of Medicine, Tokai University, Kanagawa 259-1193, Japan.

*Authors for correspondence (tkanekoi@is.icc.u-tokai.ac.jp; fishino.epgn@mri.tmd.ac.jp)

H.S., 0000-0003-2553-6971; R.O., 0000-0002-1081-0395; T.K., 0000-0002-6856-5601; T.K.-I., 0000-0002-2566-9961; F.I., 0000-0001-8458-6069; F.I., 0000-0001-8458-6069

that results in a PEG10-open reading frame (ORF) 1 and an ORF2 fusion protein (PEG10-ORF1/2), are highly conserved among all of the eutherian and marsupial orthologs of PEG10 (Shigemoto et al., 2001; Clark et al., 2007; Suzuki et al., 2007) (Fig. S1), although *PEG10* has lost the LTR sequences at both ends of its structure. These unique features, together with its emergence in therian mammals, indicate that *PEG10* was domesticated in a common therian ancestor from an extinct retrovirus ~166 million years ago (Suzuki et al., 2007; Warren et al., 2008). We previously demonstrated that *Peg10* knockout (KO) mice exhibit early embryonic lethality before 10.5 days post-coitus (dpc) owing to severe placental dysplasia, including the loss of trophoblast cells in the labyrinth and spongiotrophoblast layers (Ono et al., 2006). The labyrinth layer is an essential part of the mouse placenta in which nutrient and gas exchange occurs between the fetal and maternal blood, and trophoblast cells are unique to the placenta (Rossant and Cross, 2001). These features imply that the acquisition of *PEG10* was a crucial event in the emergence of the viviparous reproduction system in the common therian ancestor(s) (Kaneko-Ishino and Ishino, 2012, 2015).

In what manner is *PEG10* involved in placenta development? It has been reported that *PEG10* is involved in the development and progression of cancer (Okabe et al., 2003; Tsou et al., 2003; Li et al., 2006). Unfortunately, the biochemical functions of the PEG10 protein have remained obscure since its discovery in 2001, possibly because of the range of its structural and functional varieties resulting from the properties of the GAG and POL proteins. GAG and the GAG-POL fusion proteins are digested by the aspartic protease activity of POL to form several distinct parts, each with a specific role or function. These include three structural proteins (matrix, capsid and nucleocapsid proteins) from GAG along with four enzymatic proteins (aspartic protease, reverse transcriptase, RNase H and DNA integrase) from POL (Kirchner and Sandmeyer, 1993; Dunn et al., 2002; Pettit et al., 2004). Similarly, PEG10 is reported to be digested by the highly conserved aspartic protease in the POL-like ORF2 (Clark et al., 2007). Therefore, it is conceivable that PEG10 plays multiple roles during the course of development, not only in the placenta, but also in other organs and tissues. Which part and/or motif of PEG10 is essential for early placenta formation associated with trophoblast differentiation and growth, and what are the functions of other parts and/or motifs of PEG10? It is clear that a systematic approach is necessary to solve this puzzle in a step-by-step manner, so we generated a series of *Peg10* mutant mice harboring a mutation for each of the highly conserved traits. In this study, we analyzed *Peg10*-protease-motif mutant mice and found that PEG10 is expressed in the trophoblast cell layers at the feto-maternal interface and the mice exhibited perinatal lethality owing to severe defects in feto-maternal circulation in the placenta. This result clearly shows that *Peg10* plays different roles

in placental development in a stage-dependent manner – placenta formation via trophoblast differentiation and growth in the early gestational stage and maintenance of the fetal capillary network from mid- to late-gestation – and that PEG10 protease activity is indispensable for the latter process.

Interestingly, retrotransposon Gag like 1 (*RTL1*, also called *PEG11*), another paternally expressed imprinted gene, exhibits homology to the same sushi-ichi retrotransposon as *PEG10* (Charlier et al., 2001; Seitz et al., 2003; Youngson et al., 2005). It is a eutherian-specific gene and plays an essential role in the maintenance of the fetal capillary network in mid- to late-gestation on the endothelial cell side (Sekita et al., 2008; Kitazawa et al., 2017). Thus, it is likely that there exists some interaction between the two retrovirus-derived genes *Peg10* and *Rtl1*, along with their effects at the feto-maternal interface in the mouse placenta for maintaining the fetal vasculature, via their functions in trophoblast and endothelial cells, respectively.

RESULTS AND DISCUSSION

Disruption of PEG10 DSG protease activity leads to both fetal and placental growth retardation, resulting in frequent perinatal lethality

The DSG protease domain in the POL-like PEG10-ORF2 is highly conserved among therian mammals (Fig. S1), suggesting the importance of the function(s) of this domain. In an effort to determine what function the PEG10 DSG protease plays in placental development, we generated a mutant strain harboring a point mutation in the DSG domain by replacing aspartic acid (D) with an alanine (A) residue using the CRISPR-Cas9 system (Fig. 1A; Fig. S2). It has been reported that the PEG10 DSG protease exerts self-cleavage activity, producing several fragments, and that the same amino acid substitution (DSG to ASG) disrupts the protease activity of the human PEG10 protein *in vitro* (Clark et al., 2007). As *Peg10* is a paternally expressed gene, mice carrying a paternally transmitted mutant allele (+/ASG) (hereafter called *Peg10*-ASG
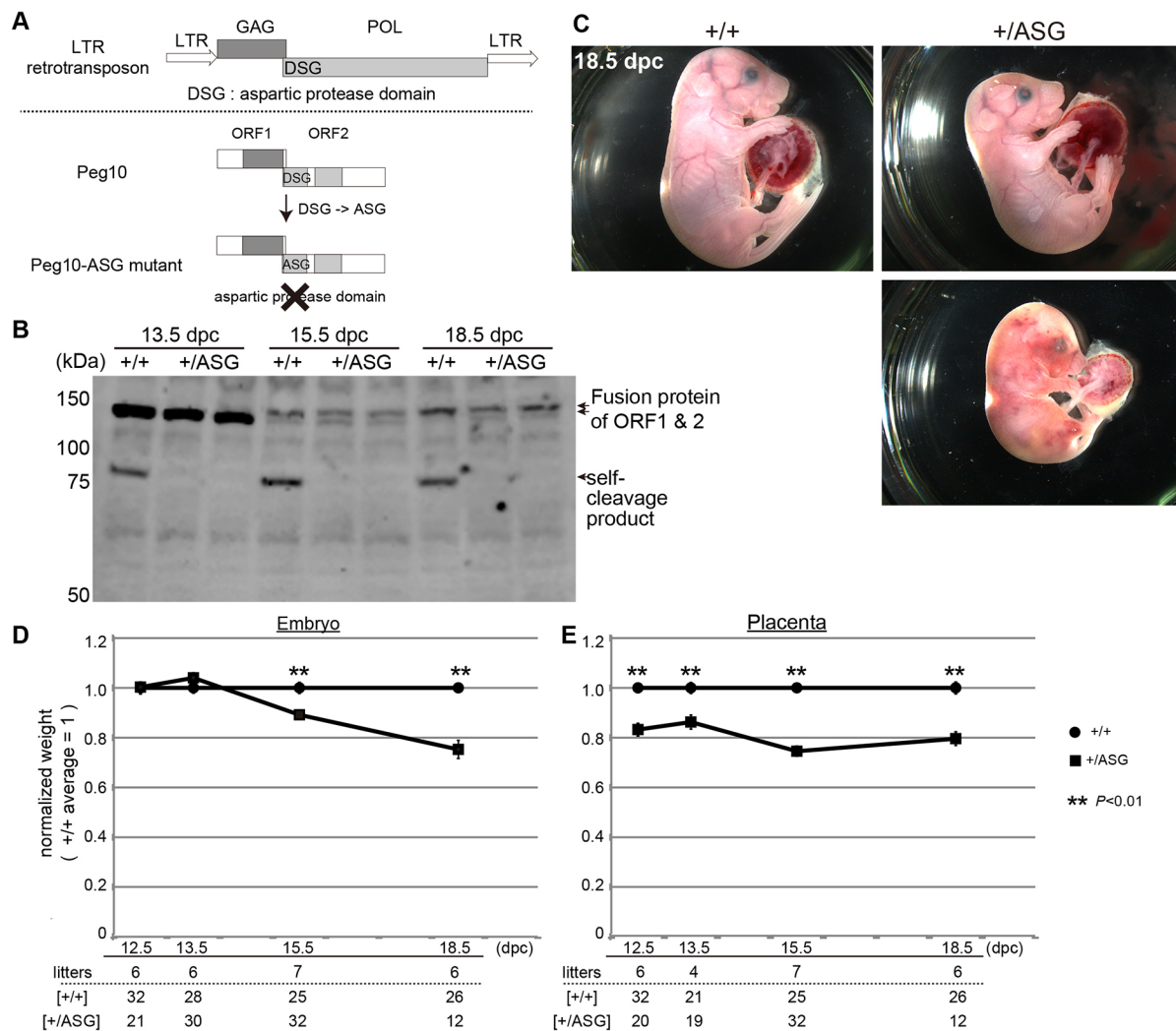

Fig. 1. Generation of *Peg10*-ASG mice harboring the PEG10 protease mutation. (A) Schematic of the *Peg10*-ASG mutation. The aspartyl protease domain composed of DSG residues was disrupted by substitution of alanine (A) for the aspartic acid (D) residue. (B) PEG10 protein expression in placenta was confirmed by using an anti-PEG10-ORF2 antibody. PEG10 self-cleaved products (~75 kDa) were undetectable in the +/ASG placentas. (C) Wild-type (+/+) (top left) and +/ASG (top right) embryos at 18.5 dpc. Some of the +/ASG embryos recovered at this stage were already dead (bottom right). (D,E) Comparison between +/+ and +/ASG embryo (D) and placental (E) weights. Mean weights were calculated for each genotype within a given litter and a value of 1 represents the mean weight of the +/+ mice. The mean±s.e.m. of each genotype were plotted. Statistical significance was calculated using a two-tailed unpaired Student's *t*-test with Welch's correction (**P<0.01).

mice) were used for phenotypic analysis throughout this study. First, we examined whether *Peg10*-ASG mice exhibit early embryonic lethality like *Peg10* null KO mice. Unexpectedly, the mutant embryos and placenta exhibited an apparently normal appearance at 12.5 dpc (Fig. S3). In western blotting experiments (Fig. 1B), a PEG10 self-cleavage product (~75 kDa) was observed only in the wild-type (+/+) placenta but was undetectable in the *Peg10*-ASG placenta, thus confirming the fact that the mutation from DSG to ASG disrupts protease activity, as expected. These results demonstrate that loss of the DSG protease function is not responsible for the early embryonic lethality associated with the

Table 1. The number of embryos or pups from +/+ dams crossed with +/ASG or ASG/+ sires

	Litters	Observed ratio +/+: +/ASG	Expected ratio (1:1)	χ^2 value	P-value
12.5 dpc	8	40 (5):29 (1)	34.5:34.5	1.75	NS (0.19)
13.5 dpc	6	28 (2):30 (0)	29:29	0.07	NS (0.79)
15.5 dpc	12	41 (3):55 (3)	48:48	2.04	NS (0.15)
18.5 dpc	12	56 (1):22 (22)	39:39	14.8	<0.0005
Weaning stage	9	30:5	17.5:17.5	17.6	<0.0001

The Chi-square test was used to determine whether the difference between an observed and expected frequency distribution (Mendelian ratio; 1:1) was statistically significant. NS, not significant. The number of dead embryos is indicated in parentheses in the 'Observed ratio' column.

differentiation and growth defects of placental trophoblast cells observed in *Peg10* null KO mice.

At the weaning stage, the total proportion of mutant pups was extremely low, only 14% (5 mutants/35 total pups) compared with the expected value of 50% (Table 1), indicating that most of the *Peg10*-ASG pups died during the course of perinatal development and growth. Approximately 50% of the recovered mutant fetuses were found dead at 18.5 dpc (22 dead fetuses/44 total fetuses) (Fig. 1C, Table 1). Moreover, the surviving mutant fetuses had small overall body size and had small placentas compared with normal mice (Fig. 1C). The mutant embryos were of normal weight before 13.5 dpc, but their growth retardation started around 15.5 dpc and reached over 20% reduction at 18.5 dpc (Fig. 1D), whereas the placental weight reduction was already evident at 12.5 dpc and persisted to term (Fig. 1E). Given that the *Peg10* expression levels are unaffected by this mutation (Fig. S4), these results demonstrate that the DSG protease activity itself is essential for placental growth in mid- to late-gestation and that the inactive ASG mutation apparently caused placental hypoplasia, which consequently led to fetal growth retardation and perinatal lethality.

Peg10-ASG mice exhibited severe defects in the vascular network in the labyrinth layer

Evident morphological abnormalities were observed in the labyrinth layers of the *Peg10*-ASG placenta. The fine, mesh-like
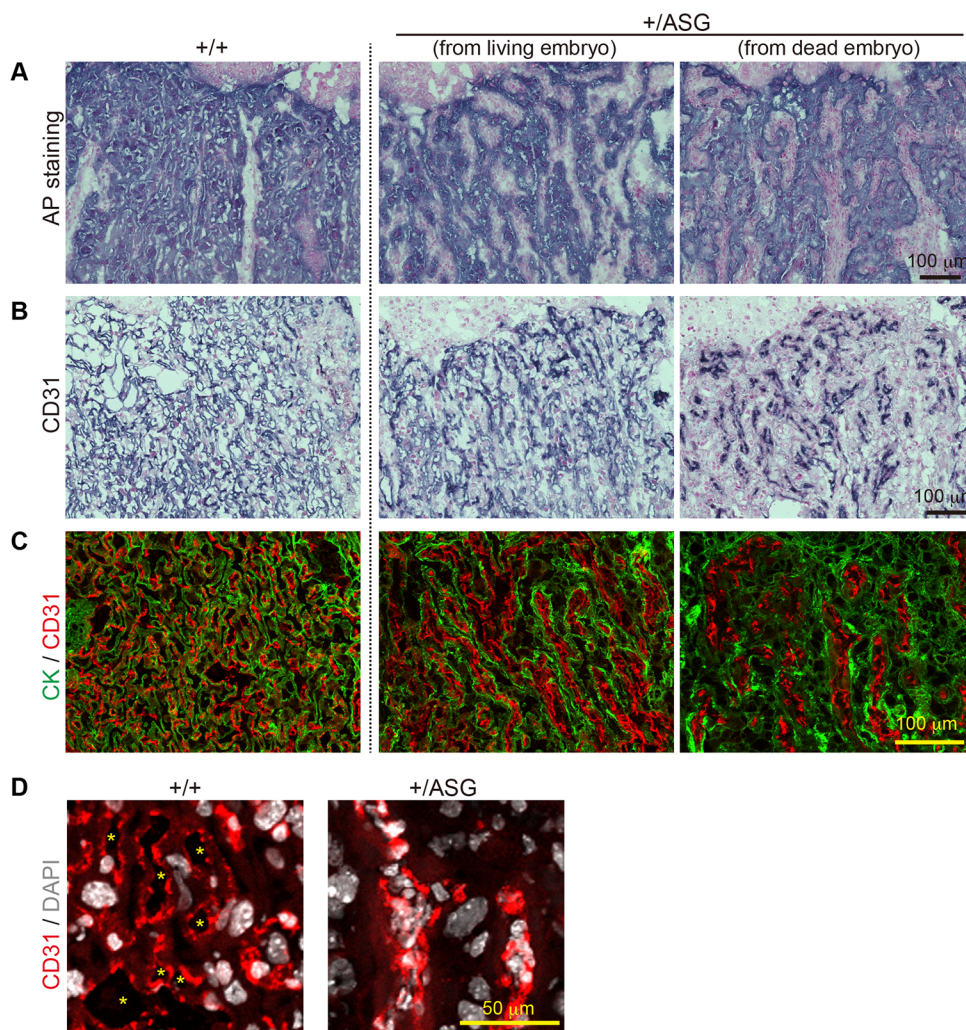

Fig. 2. Abnormal vascular organization in the +/ASG placentas. (A,B) Trophoblast cells (A) and fetal endothelial cells (B) in the labyrinth layers at 18.5 dpc were detected by alkaline phosphatase (AP) staining and immunohistochemical staining with an anti-CD31 antibody, respectively. Nuclei were stained with Nuclear Fast Red. (C) Immunofluorescence analysis of the 18.5 dpc labyrinth layers with an anti-cytokeratin (CK; trophoblast cells marker, green) and CD31 (red) antibodies. (D) Magnified images of immunofluorescence with an anti-CD31 antibody (red) and nuclear staining with DAPI (white). The asterisks indicate fetal blood spaces.

structure of the fetal vascular network was severely damaged. The fetal vasculature is composed of fetal capillary endothelial cells and three surrounding layers of trophoblast cells: two syncytiotrophoblast (SynT-I and II) layers and one mononuclear sinusoidal trophoblast giant cell (s-TGC) layer. On sections of 18.5 dpc placenta, alkaline phosphatase (AP) staining, which was employed to distinguish the maternal blood sinus (Adamson et al., 2002) (Fig. 2A; Fig. S5A), and immunohistochemistry for the endothelial marker CD31 (PECAM1) (Fig. 2B; Fig. S5B) revealed severe endothelial cell deformation and collapse of most of the fetal capillaries in the labyrinth layers, resulting in a loss of the fine, mesh-like structure of the fetal vasculature. We performed simultaneous immunofluorescence staining using antibodies against CD31 and the pan-trophoblast marker cytokeratin (CK) (Fig. 2C; Fig. S5C) to confirm a physical relationship between the fetal endothelial cells and trophoblast cells. In the normal placenta, the endothelial cells and trophoblast layers closely aligned along the fetal capillaries. In contrast, this alignment became irregular and their respective locations separated from each other in the *Peg10*-ASG placenta. Under magnified views, the fetal endothelial cell

nuclei were observed to have accumulated in narrow spaces and as a result the fetal blood spaces had become clogged (Fig. 2D; Fig. S5D). Taken together, these results suggest that abnormal organization of the fetal vasculature causes severe impairment of feto-maternal exchange in the labyrinth layer, leading to the perinatal lethality of the *Peg10*-ASG fetuses and pups.

Loss of DSG protease results in fibrinoid necrosis-like lesions in the placental labyrinth layer

Next, placental morphology was assayed by Hematoxylin and Eosin (HE) staining (Fig. 3A; Fig. S6, Fig. S7A). We found that, in addition to a significant reduction in labyrinth size (Fig. S6), the areas deeply stained in shades of pink-red containing considerable endothelial cell nuclear debris were distributed throughout the labyrinth layer in the dead mutants, and were also observed to a certain extent in the living mutants (Fig. 3A; Fig. S7A). This staining pattern showing a deposition of deep-pink pigment around the damaged capillaries is characteristically seen in one of the necrotic forms of cell death, fibrinoid necrosis (Damjanov, 2009). Additionally, immunostaining for the pan-leukocyte marker CD45
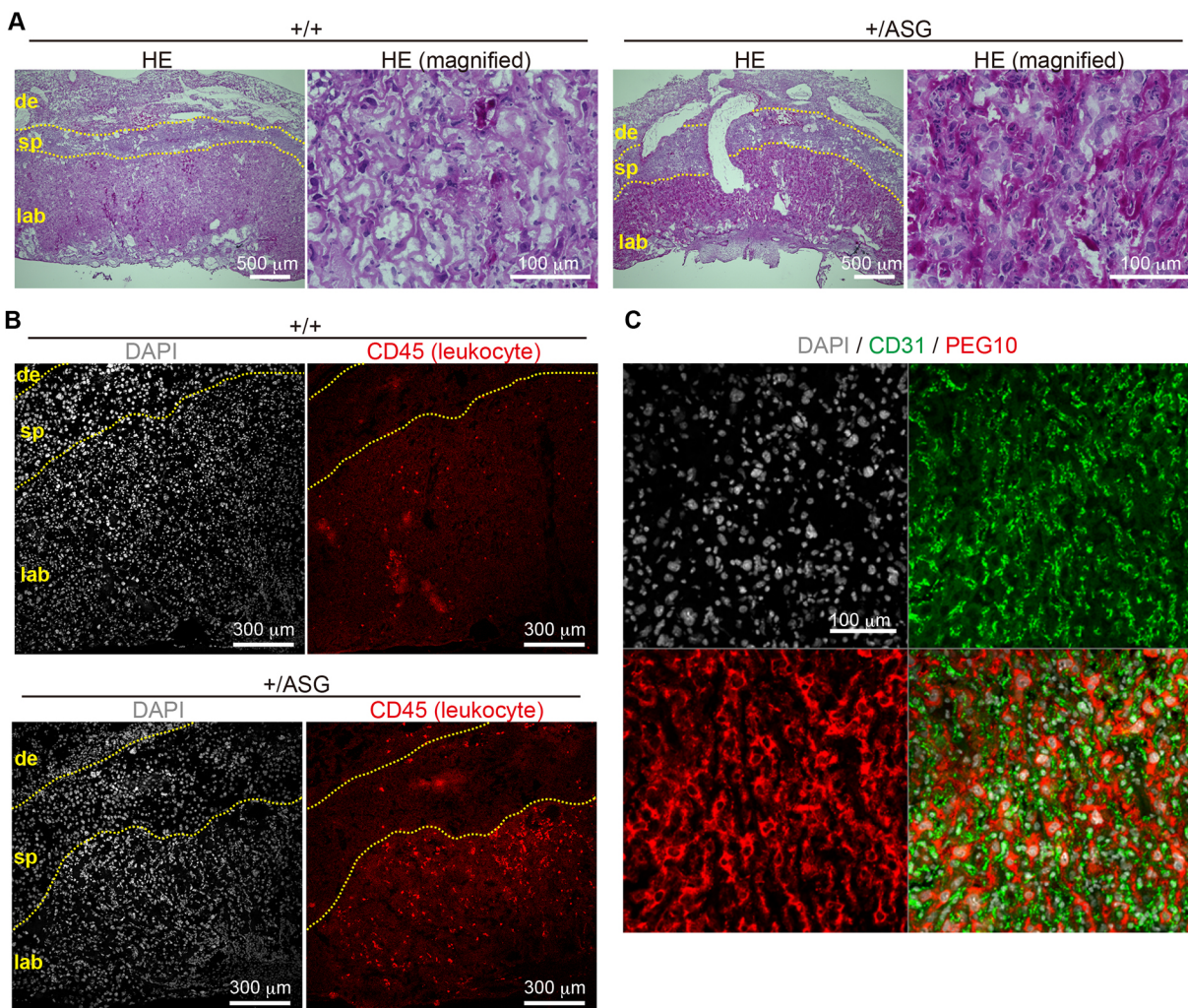

Fig. 3. The +/ASG placental labyrinth layers exhibit fibrinoid necrosis-like lesions. (A) HE-stained histological sections of 18.5 dpc placenta. Low and high magnification images of each +/+ and +/ASG placenta are represented side by side. (B) Immunofluorescence analysis of 18.5 dpc placentas with an anti-CD45 antibody (pan-leucocyte marker, red). Nuclei were stained with DAPI (white). In A,B, dotted lines indicate the borders between the maternal decidua (de) and spongiotrophoblast (sp), and between the spongiotrophoblast (sp) and labyrinth (lab) layers. (C) Immunofluorescence analysis of 18.5 dpc wild-type placenta with an anti-PEG10 (red) and CD31 (green) antibodies. Nuclei were stained with DAPI (white).

(PTPRC) revealed that the number of leukocytes was markedly increased in *Peg10*-ASG placentas obtained from deceased embryos, and a large increase in leukocytes was also observed in certain areas of the living mutant labyrinth (Fig. 3B; Fig. S7B). These results suggest that severe inflammation was induced in the fetal vasculature of the *Peg10*-ASG placenta, which then led to the development of fibrinoid necrosis-like lesions in the labyrinth layers, ultimately resulting in severe fetal damage and/or death.

Interaction between two retrovirus-derived genes at the feto-maternal interface in the eutherian placenta

In this study, it was demonstrated that the disruption of the protease activity of the DSG domain in PEG10 results in perinatal lethality associated with fetal and placental growth retardation, probably because of the severe damage inflicted on the fetal vascular network. It is likely that such extensive fetal capillary damage would result in a disturbance of the feto-maternal circulation in the placental labyrinth. This indicates that the viral-type aspartic protease domain in PEG10 is essential during the mid to late stage of placental development, implying that the protease activity that is intrinsic to the retrovirus/LTR retrotransposon was successfully domesticated (or exapted) to the placental functions in eutherians.

Importantly, as shown in Fig. S8A, PEG10 protein exhibited high expression in all layers of the placenta except for the maternal decidua, including the labyrinth layer, and expression patterns were the same in the Peg10-ASG placentas. Intriguingly, we found that PEG10 did not exhibit any localization in the CD31-positive fetal endothelial cells that were damaged in the *Peg10*-ASG placental labyrinth (Fig. 3C; Fig. S8B). Detailed analysis demonstrated that, at 12.5 dpc, the PEG10 protein signals were uniformly distributed in the region between the fetal capillaries and the maternal blood sinus, indicating that PEG10 protein was expressed in all of the trophoblast cell layers, the two syncytiotrophoblast (SynT-I and II) layers and the single s-TGC layer. After 15.5 dpc, PEG10 protein signals became prominent in cells with large nuclei facing the maternal blood sinus, which are presumed to be s-TGCs (Fig. S8B, Fig. S9). It is thus strongly suggested that the trophoblast cells in the fetal capillary, especially s-TGCs, have some defense mechanism to protect the fetal endothelial cells against non-specific hazardous events and that direct or indirect effects of PEG10 DSG protease activity is largely involved in this process. We have demonstrated in previous studies that *Rtl1* (or *Peg11*), which is derived from the presumable same retrovirus as *Peg10*, is essential for the maintenance of the fetal capillaries in the placenta (Sekita et al., 2008; Kitazawa et al., 2017). It should be noted that, in contrast to *Peg10*, *Rtl1* is only expressed in endothelial cells (Sekita et al., 2008). This demonstrates that the two retrovirus-derived genes *Peg10* and *Rtl1* function on either side of the feto-maternal interface, i.e. in trophoblasts and endothelial cells in the fetal capillaries, respectively, and presumably act in a cooperative manner in order to maintain a normal fetal vasculature for the exchange of nutrients/waste and O_2/CO_2 gas between the fetal and maternal blood (Fig. S10). Recent phylogenic analysis has revealed that the mouse and human-type hemochorial placentas, which have a feto-maternal interface in which the trophoblast surface has direct contact with the maternal blood, is ancestral eutherian placenta (Wildman et al., 2006; Roberts et al., 2016). Therefore, it is highly likely that domestication of *PEG10* and *RTL1*, before and after divergence of the eutherians and marsupials, respectively, must have been critical events and exerted a driving force in the evolution of the eutherian viviparous reproduction system via their effect on the eutherian placenta. How then do *PEG10* and *RTL1* act as

guardians of the feto-maternal interface? One possibility is that PEG10 protease activity in trophoblast cells contributes to the immune tolerance of the mother to embryo antigens: for instance, the PEG10 protease may induce an aggressiveness of trophoblasts toward maternal immune cells in order to protect the fetal capillaries. Under such a scenario, RTL1 would play a defensive role in the fetal capillary endothelial cells against a collateral attack by trophoblast cells. The cooperation between PEG10 and RTL1 would thus provide the essential architecture for the feto-maternal interface in the placenta. The trophoblast cells invariably localize between the fetal capillary endothelial cells and the maternal tissues in all three types of the eutherian placenta, the endotheliochorial (e.g. cats and dogs), epitheliochorial (e.g. horses and pigs) and hemochorial (e.g. humans and mice) placentas. They are associated with invasiveness and access to maternal blood flow (Nakaya and Miyazawa, 2015; Roberts et al., 2016). The fact that the protease domain in PEG10 is highly conserved in all eutherian species (Fig. S1) suggests that the protease activity of PEG10 plays an important role. Accordingly, the relationship between PEG10 and RTL1 evolved to provide an adequate feto-maternal interface in a placental type-specific manner. Future studies are needed to determine the molecular mechanisms by which *PEG10* and *RTL1* exert a cooperatively beneficial effect on protecting the fetal capillaries via their crucial involvement in the immune tolerance system during pregnancy.

PEG10 and *RTL1* are expressed in many other tissues and organs besides the placenta (Abed et al., 2019; Kitazawa et al., 2021). Recently, we demonstrated that mouse *Rtl1* plays other important roles during the course of development, such as in fetal/neonatal skeletal muscle maturation as well as in functional activity of the central nervous system (Kitazawa et al., 2020, 2021). Therefore, it is possible that *PEG10* has a multiplicity of functions across a range of organs and tissues. Future studies are needed to show how *PEG10* contributed to the evolution and acquisition of various other therian-specific traits, and it may turn out that both *PEG10* and *RTL1* were domesticated in the same process and function cooperatively in current eutherian developmental systems, as in the case of the maintenance of the fetal vascular network in the placenta.

MATERIALS AND METHODS
Mice
All animal and experimental procedures were approved by the Animal Ethics Committees of Tokyo Medical and Dental University and the University of Yamanashi. Animals were allowed access to a standard chow diet and water *ad libitum* and were housed in a pathogen-free barrier facility with a 12:12 h light-dark cycle.

Plasmid preparation
The plasmids expressing *hCas9* and sgRNA were prepared by ligating oligos into the BbsI site of pX330 (Addgene plasmid #42230). The 20 bp sgRNA recognition sequence was:

Peg10-ORF2-sgRNA (5′-GTCCGAGCTATGATTGATTC-3′).

The oligo DNA for co-injection with the plasmid into mouse zygotes was:
ACCTGCAAGTGATGCTCCAGATTCATATGCCGGGCAGACCCAC-CCTGTTTGTCCGAGCTATGATTG**C**TTCTGGTGCATCTGGCAACTT-CATTGATCAAGACTTTGTCATACAAAATGCAATTCCTCTCAGAAT.

Production of *hCas9* mRNA and *Peg10*-ORF1-sgRNA
To produce the *hCas9* mRNA, the T7 promoter was added to the *hCas9* coding region of the pX330 plasmid by PCR amplification, as previously reported (Wang et al., 2013). The T7-*Cas9* PCR product was gel-purified and used as the template for *in vitro* transcription (IVT) using the mMESSAGE mMACHINE T7 ULTRA kit (Life Technologies). The T7

promoter was added to the *Peg10*-ORF2-sgRNA region of the pX330 plasmid by PCR amplification using the following primers:

Peg10-ORF2-IVT-F, TTAATACGACTCACTATAGGTCCGAGCTAT-GATTGATTC; IVT-R, AAAAGCACCGACTCGGTGCC.

The T7-sgRNA PCR product was gel-purified and employed as the template for IVT using the MEGAshortscript T7 kit (Life Technologies). Both the *Cas9* mRNA and *Peg10*-ORF2-sgRNA were DNase-treated to eliminate template DNA, purified using the MEGAclear kit (Life Technologies), and eluted into RNase-free water.

Generation of *Peg10*-ASG mice
B6D2F1 female mice were superovulated and *in vitro* fertilization was carried out using B6D2F1 mouse sperm. The synthesized *hCas9* mRNA (50 ng/μl) and *Peg10*- ORF2-sgRNA (25 ng/μl) with oligo DNA (10 ng/μl) were injected into the cytoplasm of fertilized eggs at the indicated concentration. The eggs were cultivated in KSOM overnight, then transferred into the oviducts of pseudopregnant ICR females. The genotype was determined by direct sequencing of the PCR product using the following primers: F primer, GGAAGGTCTCAACCCAGACA; R primer, GTATCTCACGGTGGTCTCCC. The F-primer was used for direct sequencing.

Real-time quantitative PCR
The assays were performed in triplicate and the copy number of the genes examined was calculated with a StepOnePlus Real Time PCR system (Thermo Fisher Scientific) using the THUNDERBIRD SYBR qPCR Mix (TOYOBO). PCR was carried out under the following conditions: 95°C for 15 s, 65°C for 30 s and 72°C for 30 s. The primers used are as follows:

Peg10-F, TTGGTCCCTTACCCCTACCAAC; *Peg10*-R, CCCTTGA-GTTAATTCCCAGAGCC; *Actb*-F, AAGTGTGACGTTGACATCCG; *Actb*-R, GATCCACATCTGCTGGAAGG.

Preparation of frozen sections
The recovered mouse placentas were directly embedded in OCT compound (Sakura Finetek) or first fixed in 4% paraformaldehyde, incubated sequentially in 10% sucrose in PBS for 2 h, 15% sucrose in PBS for 2 h then 25% sucrose in PBS overnight at 4°C, and ultimately embedded in OCT compound (Sakura Finetek). The OCT blocks were sectioned at a thickness of 7 μm with a cryostat (Thermo Fisher Scientific) and mounted on Superfrost Micro Slides (Matsunami Glass).

Generation of antibodies
Anti-PEG10-ORF1 antibody was generated according to the protocol of the iliac lymph node method (Kishiro et al., 1995). Briefly, after immunizing with the whole PEG10-ORF1 via rat hind footpads for 3 weeks, cells from iliac lymph node were fused with SP2/O-Ag14 mouse myeloma cells. Cell lines with high ability for anti-PEG10-ORF1 antibody production were then screened. The specificity of anti-PEG10-ORF1 antibody in immunofluorescence analysis was validated by using the tissues from Peg10 null KO mice as a true negative control for our experiments. Anti-PEG10-ORF2 antibody was produced from rabbit serum by immunizing with the synthetic PEG10 peptide (NH2-CPSGHLYSMSESEMN-COOH) and purified by antigen-specific affinity purification. The antibodies were validated in a western blot by checking whether the band size was generally consistent with the expected molecular weight and using the lysate from Peg10 null KO cells as a true negative control for our western blot analysis.

Histological analysis
Frozen sections were fixed in 4% paraformaldehyde for 10 min at room temperature and washed three times with PBS for 5 min. The sections were then subjected to HE staining, immunodetection (immunofluorescence and immunohistochemistry) or endogenous alkaline phosphatase activity detection.

For HE staining, the sections were stained with HE, and mounted with Malinol mounting medium (Muto Pure Chemicals).

For immunodetection, after incubation in blocking buffer (1% bovine serum albumin in PBS with 0.1% Triton X-100) for 60 min, the sections were reacted with primary antibody in blocking buffer at 4°C overnight.

Primary antibodies used were: rat monoclonal anti-CD31 (1:100; BD Biosciences, 550274), rabbit polyclonal anti-CD31 (1:50; Abcam, ab28364) or rabbit recombinant multiclonal anti-CD31 (1:100; Abcam, ab281583); rabbit polyclonal anti-cytokeratin (1:200; Dako, Z0622); rat monoclonal anti-CD45 (1:100; BD Biosciences, 561037); rat monoclonal anti-PEG10-ORF1 (1:200; produced in-house). After washing with PBS three times for 5 min each, the sections were incubated with a secondary antibody conjugated with a fluorescence label for immunofluorescence [goat anti-rat IgG conjugated with Cy3 (1:500; Thermo Fisher Scientific, A10522) or goat anti-rabbit IgG conjugated with Alexa 488 (1:500; Thermo Fisher Scientific, A11008)] or biotin for immunohistochemistry [donkey anti-rat IgG conjugated with biotin (1:500; Jackson ImmunoResearch, 712-065-153)] in blocking buffer at 4°C overnight. For immunofluorescence, after washing with PBS three times for 5 min each, the slides were mounted with VECTASHIELD-Hardset (Vector Laboratories) containing 1 μg/ml DAPI. The sections were imaged under confocal or widefield fluorescence microscopy (LSM510, Carl Zeiss; or EVOS M5000, Thermo Fisher Scientific). For immunohistochemistry, after washing with PBS three times for 5 min each, the slides were incubated with ABC-AP reagent (VECTASTAIN ABC-AP Kit, Vector Laboratories) with 200 nM levamisole for 30 min at room temperature. The sides were washed in PBS, followed by incubation with 100 mM Tris-HCl (pH 9.5) for 10 min at room temperature. Chromogenic detection was performed by NBT-BCIP staining (BCIP/NBT AP substrate, Vector Laboratories) according to the manufacturer's instructions. After rinsing with 100 mM Tris-HCl (pH 9.5), the sections were counterstained with Nuclear Fast Red (Vector Laboratories). For endogenous alkaline phosphatase activity detection, after being incubated with 100 mM Tris-HCl (pH 9.5) for 10 min at room temperature, chromogenic detection was performed as described above.

Western blot analysis
Placenta tissue lysates were resolved by SDS-PAGE and transferred to a PVDF membrane (Bio-Rad) before immunoblotting. The membrane was then probed with the rabbit polyclonal anti-Peg10-ORF2 antibody (1:1000; produced in-house), followed by incubation with horseradish peroxidase-conjugated donkey anti-rabbit IgG (1:5000; GE Healthcare, NA9340). The blots were developed using the ECL system according to the manufacturer's instructions (Thermo Fisher Scientific).

References
Abed, M., Verschueren, E., Budayeva, H., Liu, P., Kirkpatrick, D. S., Reja, R., Kummerfeld, S. K., Webster, J. D., Gierke, S., Reichelt, M. et al. (2019). The Gag protein PEG10 binds to RNA and regulates trophoblast stem cell lineage specification. *PLoS ONE* **14**, e0214110. doi:10.1371/journal.pone.0214110

Adamson, S. L., Lu, Y., Whiteley, K. J., Holmyard, D., Hemberger, M., Pfarrer, C. and Cross, J. C. (2002). Interactions between trophoblast cells and the maternal and fetal circulation in the mouse placenta. *Dev. Biol.* **250**, 358-373. doi:10.1006/dbio.2002.0773

Charlier, C., Segers, K., Wagenaar, D., Karim, L., Berghmans, S., Jaillon, O., Shay, T., Weissenbach, J., Cockett, N., Gyapay, G. et al. (2001). Human-ovine comparative sequencing of a 250-kb imprinted domain encompassing the callipyge (clpg) locus and identification of six imprinted transcripts: DLK1, DAT, GTL2, PEG11, antiPEG11, and MEG8. *Genome Res.* **11**, 850-862. doi:10.1101/gr.172701

Clark, M. B., Jänicke, M., Gottesbühren, U., Kleffmann, T., Legge, M., Poole, E. S. and Tate, W. P. (2007). Mammalian gene PEG10 expresses two reading frames by high efficiency −1 frameshifting in embryonic-associated tissues. *J. Biol. Chem.* **282**, 37359-37369. doi:10.1074/jbc.M705676200

Damjanov, I. (2009). *Pathology Secrets*. Philadelphia, PA: Mosby/Elsevier.

Dunn, B. M., Goodenow, M. M., Gustchina, A. and Wlodawer, A. (2002). Retroviral proteases. *Genome Biol.* **3**, reviews3006.1. doi:10.1186/gb-2002-3-4-reviews3006

Kaneko-Ishino, T. and Ishino, F. (2012). The role of genes domesticated from LTR retrotransposons and retroviruses in mammals. *Front. Microbiol.* **3**, 262. doi:10.3389/fmicb.2012.00262.

Kaneko-Ishino, T. and Ishino, F. (2015). Mammalian-specific genomic functions: newly acquired traits generated by genomic imprinting and LTR retrotransposon-derived genes in mammals. *Proc. Jpn. Acad. Ser. B* **91**, 511-538. doi:10.2183/pjab.91.511

Kirchner, J. and Sandmeyer, S. (1993). Proteolytic processing of Ty3 proteins is required for transposition. *J. Virol.* **67**, 19-28. doi:10.1128/jvi.67.1.19-28.1993

Kishiro, Y., Kagawa, M. and Sado, Y. (1995). A novel method of perparing rat-monoclonal antibody-producing hybridomas by using rat medial iliac lymph node cells. *Cell Struct. Funct.* **20**, 151-156. doi:10.1247/csf/30.151

Kitazawa, M., Tamura, M., Kaneko-Ishino, T. and Ishino, F. (2017). Severe damage to the placental fetal capillary network causes mid- to late fetal lethality and reduction in placental size in Peg11/Rtl1 KO mice. *Genes Cells* **22**, 174-188. doi:10.1111/gtc.12465

Kitazawa, M., Hayashi, S., Imamura, M., Takeda, S., Oishi, Y., Kaneko-Ishino, T. and Ishino, F. (2020). Deficiency and overexpression of Rtl1 in the mouse cause distinct muscle abnormalities related to temple and kagami-ogata syndromes. *Development* **147**, dev185918. doi:10.1242/dev.185918

Kitazawa, M., Sutani, A., Kaneko-Ishino, T. and Ishino, F. (2021). The role of eutherian-specific RTL1 in the nervous system and its implications for the Kagami-Ogata and temple syndromes. *Genes Cells* **26**, 165-179. doi:10.1111/gtc.12830

Li, C.-M., Margolin, A. A., Salas, M., Memeo, L., Mansukhani, M., Hibshoosh, H., Szabolcs, M., Klinakis, A. and Tycko, B. (2006). PEG10 is a c-MYC target gene in cancer cells. *Cancer Res.* **66**, 665-672. doi:10.1158/0008-5472.CAN-05-1553

Nakaya, Y. and Miyazawa, T. (2015). The roles of syncytin-like proteins in ruminant placentation. *Viruses* **7**, 2928-2942. doi:10.3390/v7062753

Okabe, H., Satoh, S., Furukawa, Y., Kato, T., Hasegawa, S., Nakajima, Y., Yamaoka, Y. and Nakamura, Y. (2003). Involvement of PEG10 in human hepatocellular carcinogenesis through interaction with SIAH1. *Cancer Res.* **63**, 3043-3048.

Ono, R., Kobayashi, S., Wagatsuma, H., Aisaka, K., Kohda, T., Kaneko-Ishino, T. and Ishino, F. (2001). A retrotransposon-derived gene, PEG10, is a novel imprinted gene located on human chromosome 7q21. *Genomics* **73**, 232-237. doi:10.1006/geno.2001.6494

Ono, R., Nakamura, K., Inoue, K., Naruse, M., Usami, T., Wakisaka-Saito, N., Hino, T., Suzuki-Migishima, R., Ogonuki, N., Miki, H. et al. (2006). Deletion of Peg10, an imprinted gene acquired from a retrotransposon, causes early embryonic lethality. *Nat. Genet.* **38**, 101-106. doi:10.1038/ng1699

Pettit, S. C., Everitt, L. E., Choudhury, S., Dunn, B. M. and Kaplan, A. H. (2004). Initial cleavage of the human immunodeficiency virus type 1 GagPol precursor by its activated protease occurs by an intramolecular mechanism. *J. Virol.* **78**, 8477-8485. doi:10.1128/JVI.78.16.8477-8485.2004

Roberts, R. M., Green, J. A. and Schulz, L. C. (2016). The evolution of the placenta. *Reproduction* **152**, R179-R189. doi:10.1530/REP-16-0325

Rossant, J. and Cross, J. C. (2001). Placental development: lessons from mouse mutants. *Nat. Rev. Genet.* **2**, 538-548. doi:10.1038/35080570

Seitz, H., Youngson, N., Lin, S.-P., Dalbert, S., Paulsen, M., Bachellerie, J.-P., Ferguson-Smith, A. C. and Cavaillé, J. (2003). Imprinted microRNA genes transcribed antisense to a reciprocally imprinted retrotransposon-like gene. *Nat. Genet.* **34**, 261-262. doi:10.1038/ng1171

Sekita, Y., Wagatsuma, H., Nakamura, K., Ono, R., Kagami, M., Wakisaka, N., Hino, T., Suzuki-Migishima, R., Kohda, T., Ogura, A. et al. (2008). Role of retrotransposon-derived imprinted gene, Rtl1, in the feto-maternal interface of mouse placenta. *Nat. Genet.* **40**, 243-248. doi:10.1038/ng.2007.51

Shigemoto, K., Brennan, J., Walls, E., Watson, C. J., Stott, D., Rigby, P. W. J. and Reith, A. D. (2001). Identification and characterisation of a developmentally regulated mammalian gene that utilises −1 programmed ribosomal frameshifting. *Nucleic Acids Res.* **29**, 4079-4088. doi:10.1093/nar/29.19.4079

Suzuki, S., Ono, R., Narita, T., Pask, A. J., Shaw, G., Wang, C., Kohda, T., Alsop, A. E., Marshall Graves, J. A., Kohara, Y. et al. (2007). Retrotransposon silencing by DNA methylation can drive mammalian genomic imprinting. *PLoS Genet.* **3**, e55. doi:10.1371/journal.pgen.0030055

Tsou, A.-P., Chuang, Y.-C., Su, J.-Y., Yang, C.-W., Liao, Y.-L., Liu, W.-K., Chiu, J.-H. and Chou, C.-K. (2003). Overexpression of a novel imprinted gene, PEG10, in human hepatocellular carcinoma and in regenerating mouse livers. *J. Biomed. Sci.* **10**, 625-635. doi:10.1007/BF02256313

Wang, H., Yang, H., Shivalila, C. S., Dawlaty, M. M., Cheng, A. W., Zhang, F. and Jaenisch, R. (2013). One-step generation of mice carrying mutations in multiple genes by CRISPR/Cas-mediated genome engineering. *Cell* **153**, 910-918. doi:10.1016/j.cell.2013.04.025

Warren, W. C., Hillier, L. W., Marshall Graves, J. A., Birney, E., Ponting, C. P., Grutzner, F., Belov, K., Miller, W., Clarke, L., Chinwalla, A. T. et al. (2008). Genome analysis of the platypus reveals unique signatures of evolution. *Nature* **453**, 175-183. doi:10.1038/nature06936

Wildman, D. E., Chen, C., Erez, O., Grossman, L. I., Goodman, M. and Romero, R. (2006). Evolution of the mammalian placenta revealed by phylogenetic analysis. *Proc. Natl. Acad. Sci. USA* **103**, 3203-3208. doi:10.1073/pnas.0511344103

Youngson, N. A., Kocialkowski, S., Peel, N. and Ferguson-Smith, A. C. (2005). A small family of sushi-class retrotransposon-derived genes in mammals and their relation to genomic imprinting. *J. Mol. Evol.* **61**, 481-490. doi:10.1007/s00239-004-0332-0
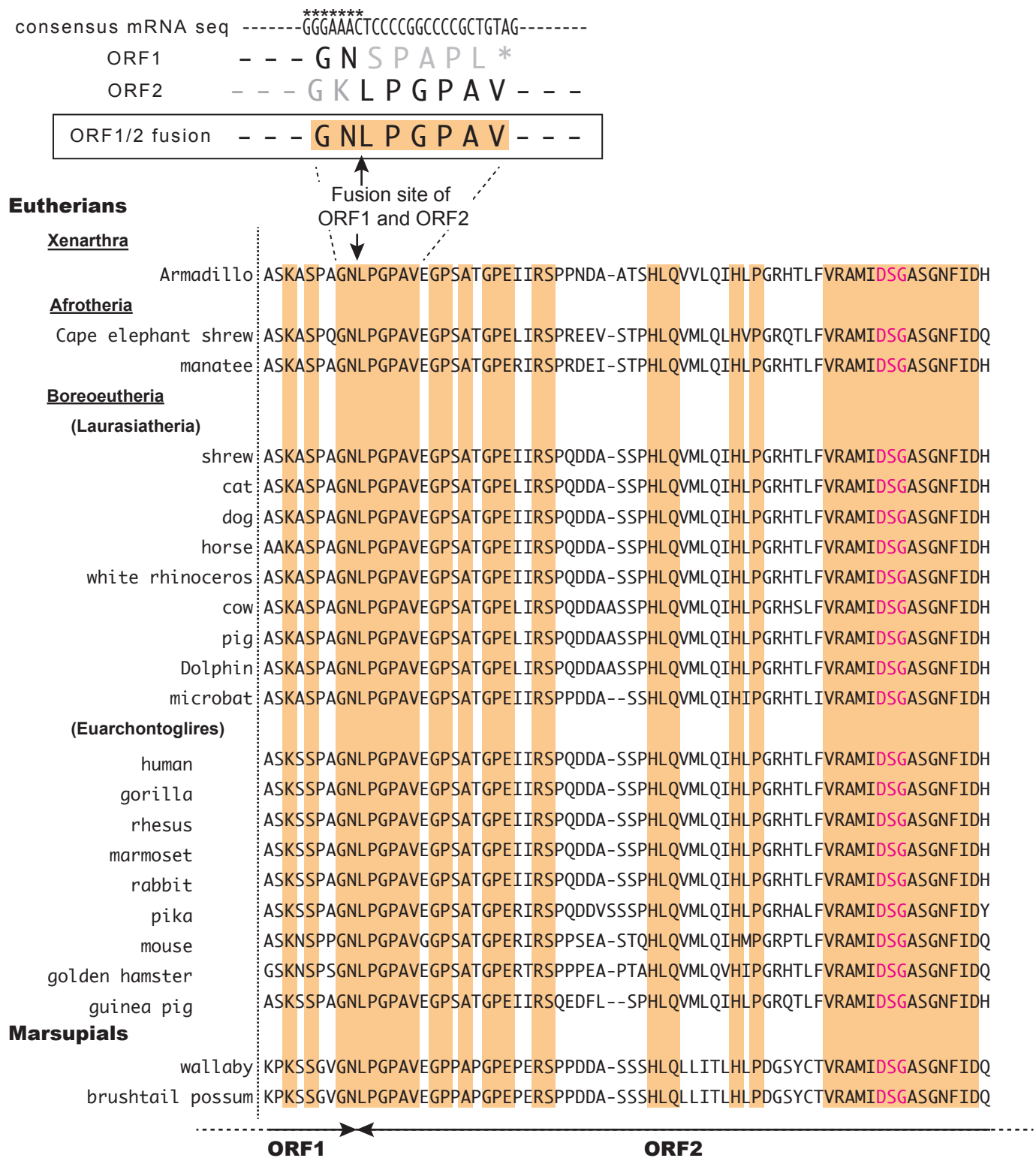
Fig. S1. The PEG10 ORF1/2 fusion protein and its DSG viral aspartic protease motif are highly conserved among all of the therian mammals.

Top: *PEG10* has a consensus slippery sequence, GGGAAAC (=XXXYYYZ) that is essential for the -1 frameshift that results in an ORF1/2 fusion protein between the ORF1 C-terminus and the head of ORF2. Bottom: Conservation of the amino acid sequence of the ORF1/2 fusion region as well as the conserved DSG protease motif (shown in red) in the ORF2 in the eutherian and marsupial species, indicating the importance of the ORF1/2 fusion protein and its protease activity.
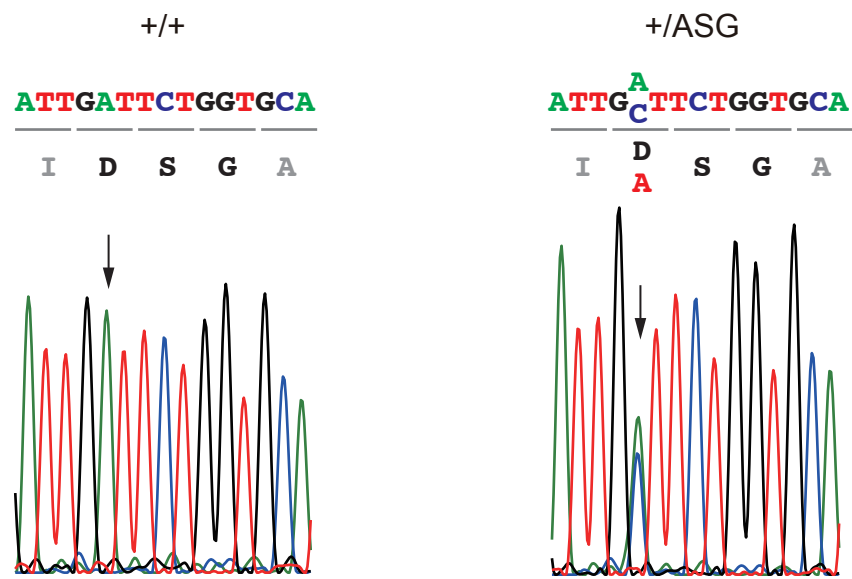
Fig. S2. Genotyping of the +/+ and +/ASG mice.

A point mutation, A to C, results in the amino acid substitution, <u>D</u>SG to <u>A</u>SG, in +/ASG mice.
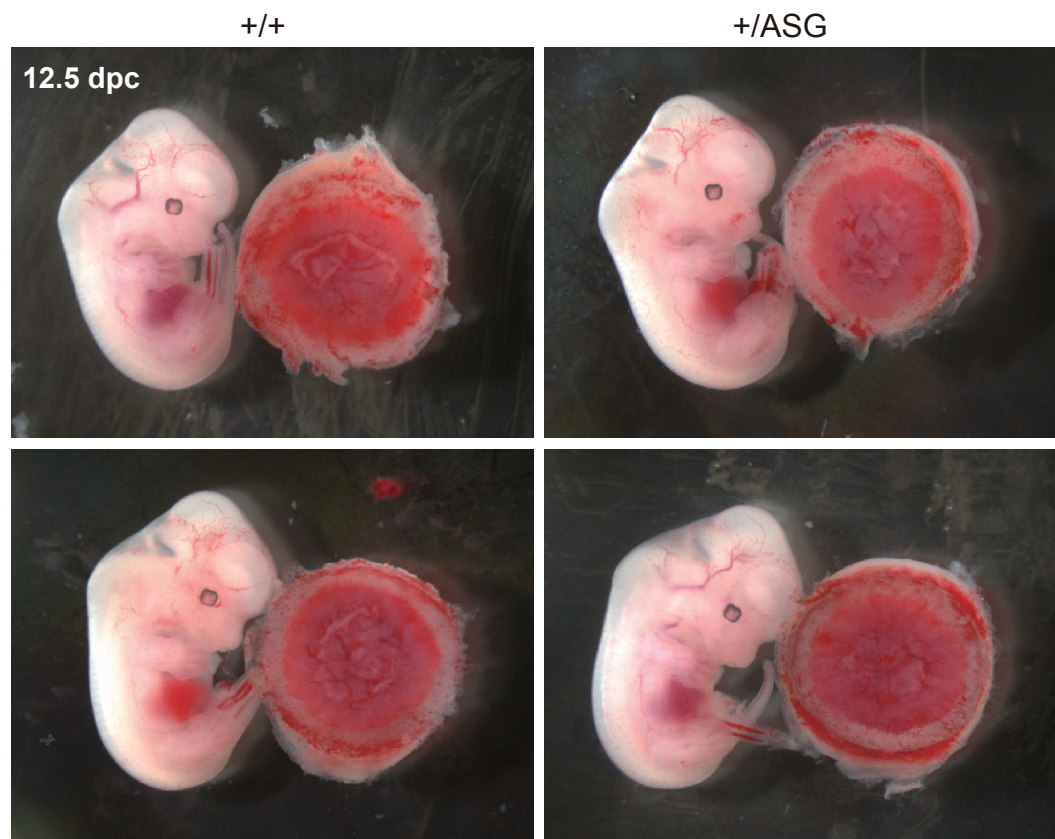
Fig. S3. Both embryos and placentas of *Peg10*-ASG are apparently normal at 12.5 dpc.+/
+ (left) and +/ASG (right) embryos are shown along with their placentas at 12.5 dpc.
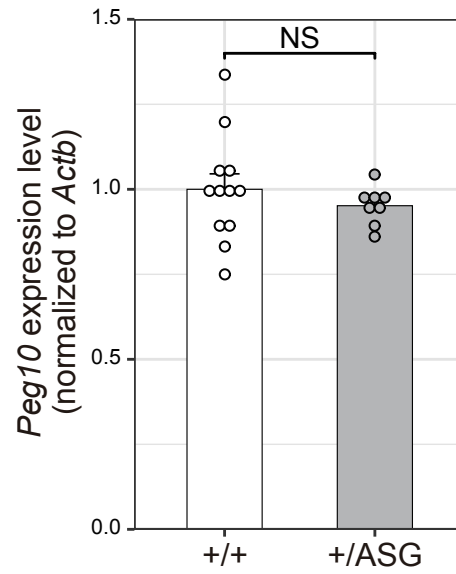
Fig. S4. *Peg10* expression level in 12.5 dpc placenta.
The *Peg10* expression level was determined by quantitative PCR analysis. The value of '1' represents the mean *Peg10* expression level in the +/+ placenta. In total 20 samples from two litters (+/+ : +/ASG = 12 : 8) were examined. The mean values of each genotype were plotted and each dot indicates the value obtained from each sample. Statistical significance was calculated using a two-tailed unpaired Student's t-test with Welch's correction. The error bars indicate the s.e.m. NS; Not significant.

A

B

+/+
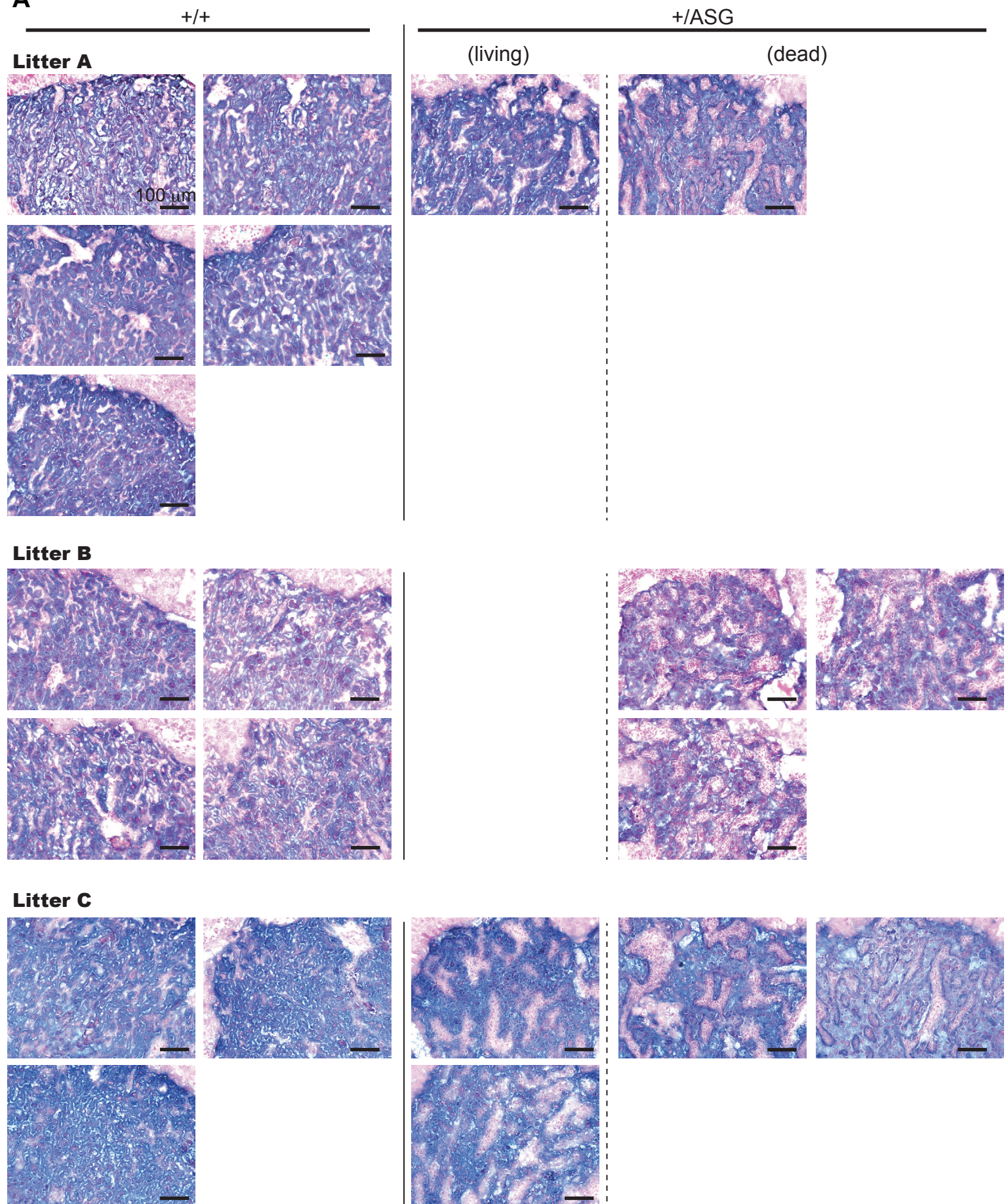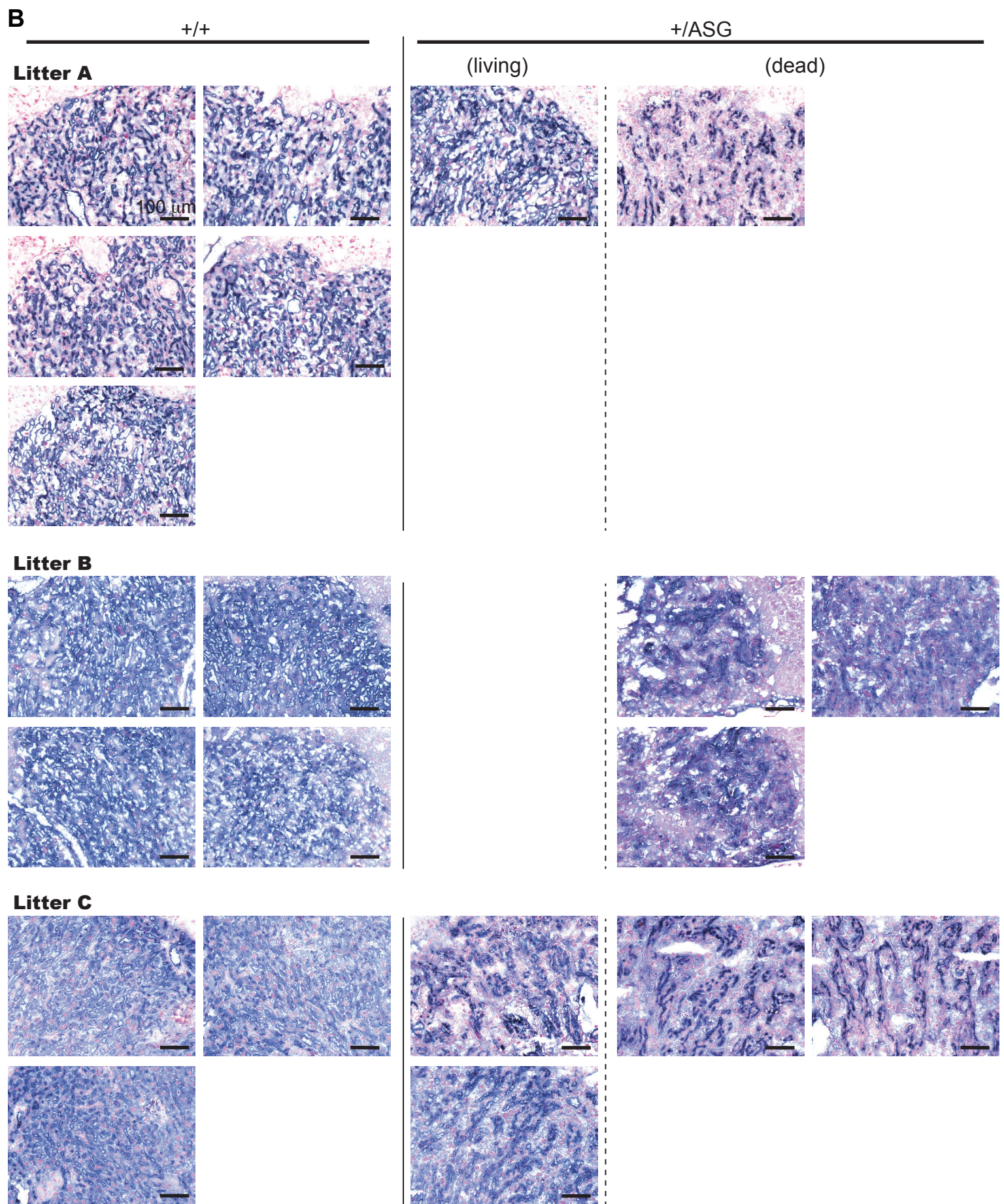
+/ASG
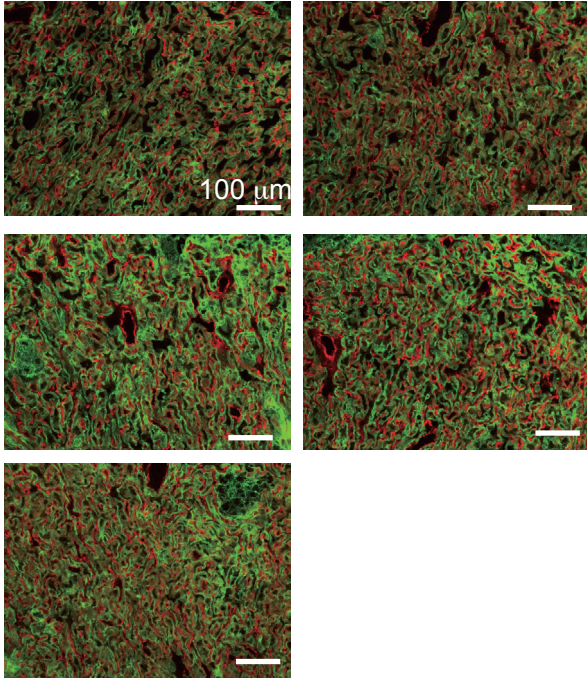
Litter A

(living)

(dead)

Litter B

Litter C

C

+/+ +/ASG

(living) (dead)

Litter A

100 µm
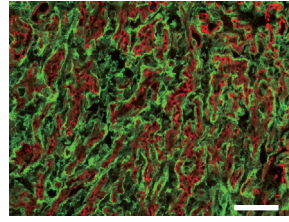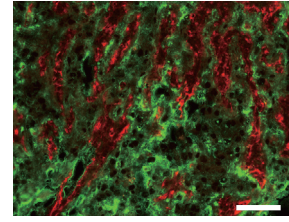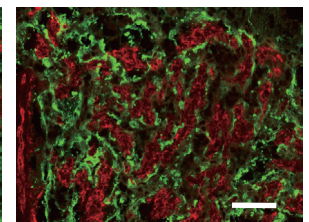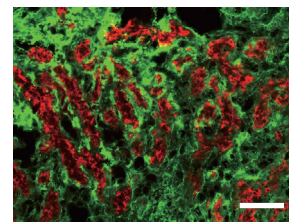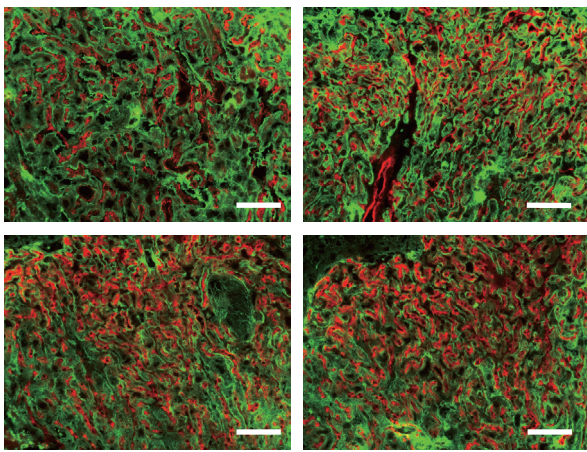
Litter B

Litter D
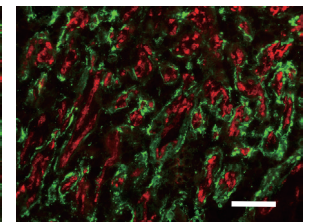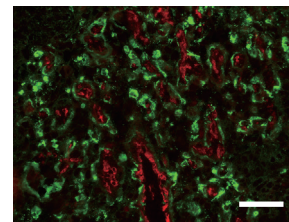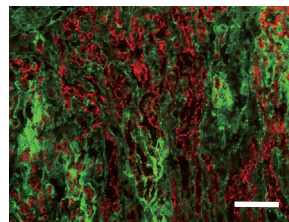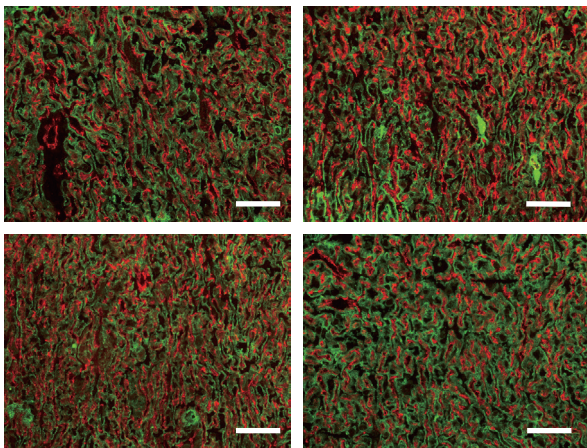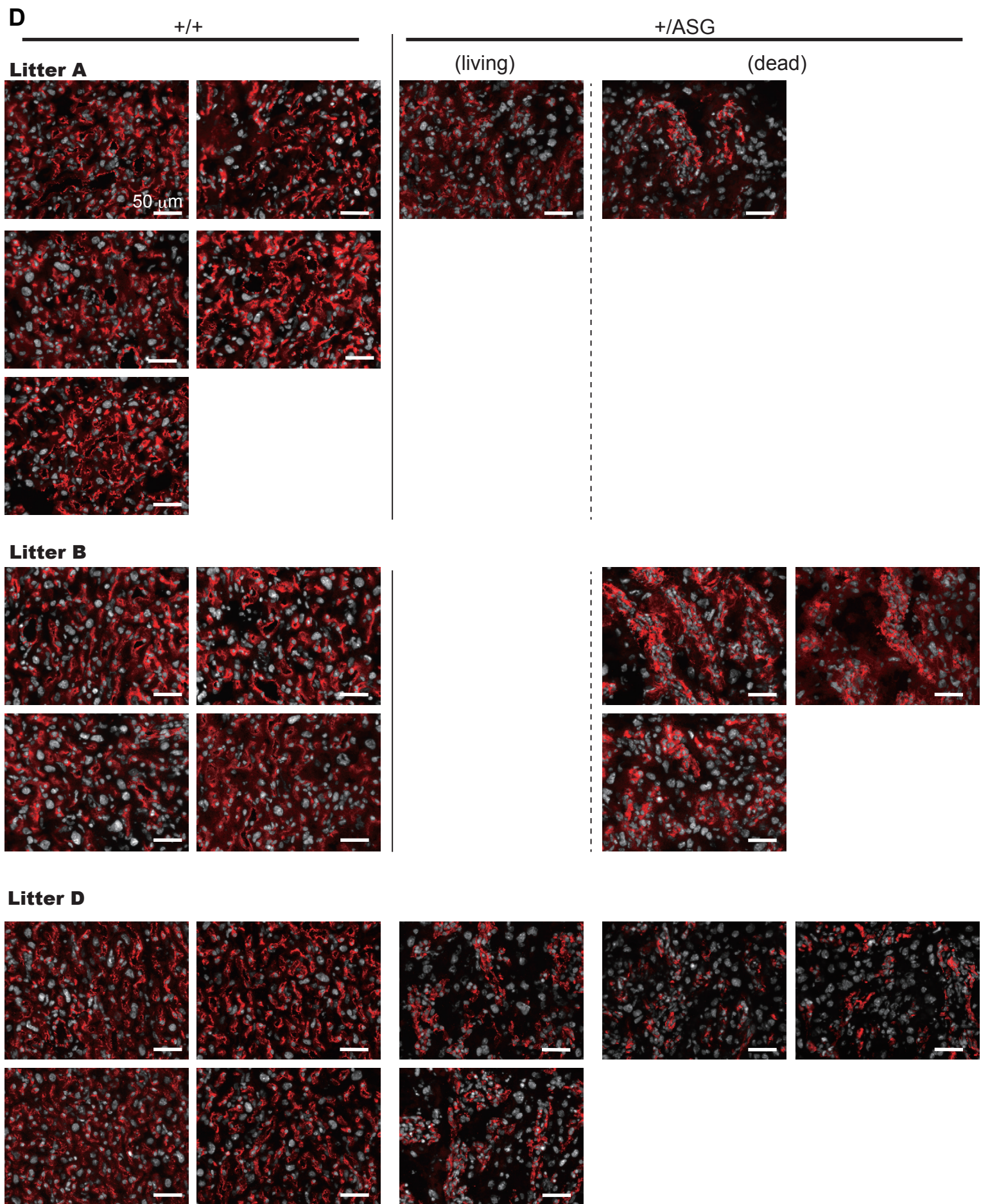
Fig. S5. Additional images related to Figure 2.

(A) Alkaline phosphatase (AP) staining and (B) immunohistochemical staining with an anti-CD31 antibody of the 18.5 dpc labyrinth layers, respectively. Nuclei were stained with Nuclear Fast Red. (C) Immunofluorescence analysis of the 18.5 dpc labyrinth layers with an anti-cytokeratin (CK) (green) and CD31 (red) antibodies. (D) Magnified images of the immunofluorescence with an anti-CD31 antibody (red) and nuclear staining with DAPI (white). For each analysis, all of the placentas recovered from three litters were examined.
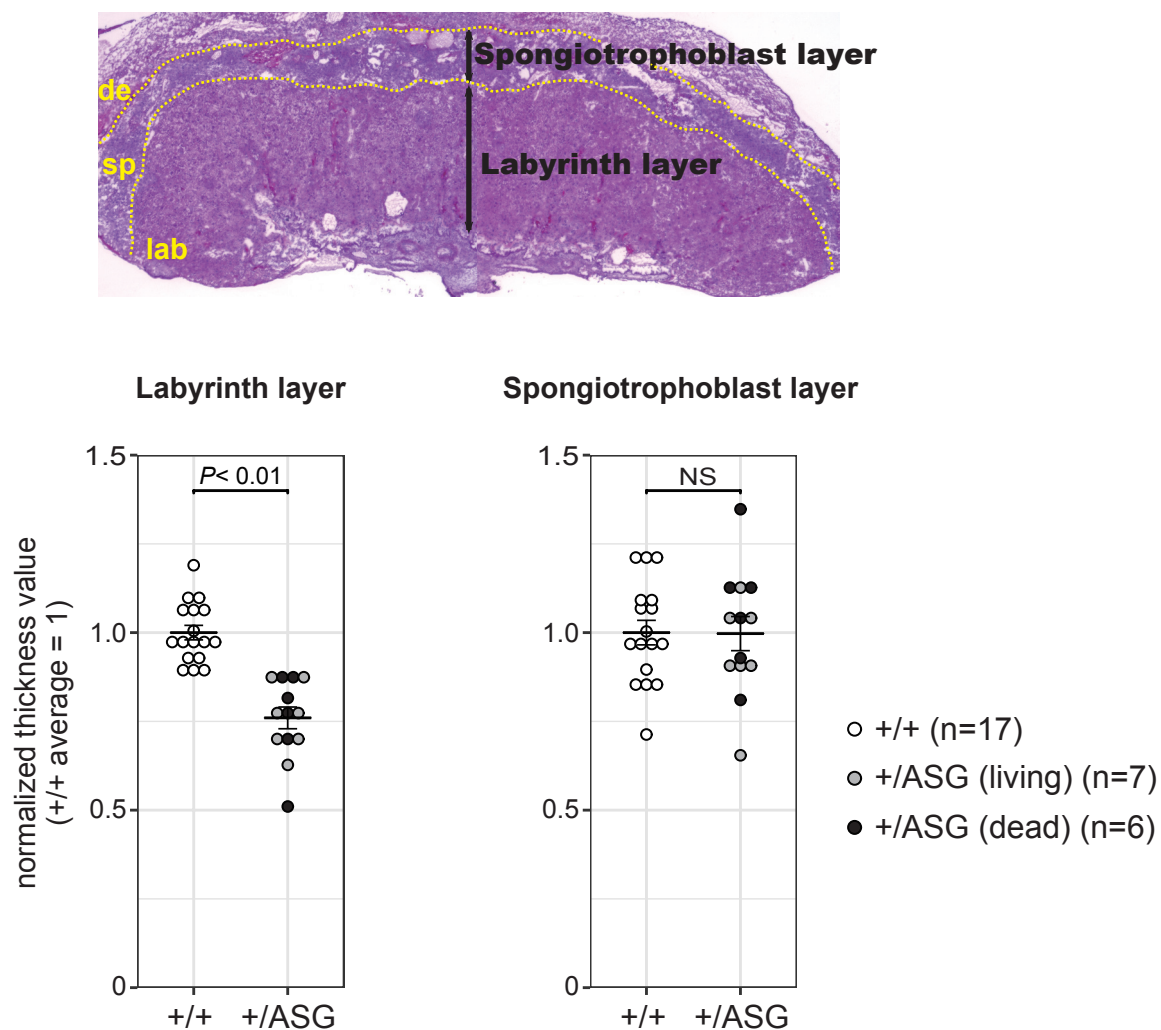
Fig. S6. Analysis of the size of labyrinth and spongiotrophoblast layers.
The thickness of the labyrinth and spongiotrophoblast layers in the +/+ and +/ASG placenta at 18.5 dpc was examined. In total, 30 placentas from four litters were used for this analysis. A value of 1 represents the mean thickness of the +/+ mice. The lines within the graphs indicate the mean values for each genotype and each dot represents the value for each placenta. Statistical significance was calculated using a two-tailed unpaired Student's t-test with Welch's correction. The error bars indicate the s.e.m. NS; Not significant. The top image is a representative image of a HE stained placenta. The dotted lines indicate the borders between the maternal decidua (de) and spongiotrophoblast (sp), and between the spongiotrophoblast (sp) and labyrinth (lab) layers.
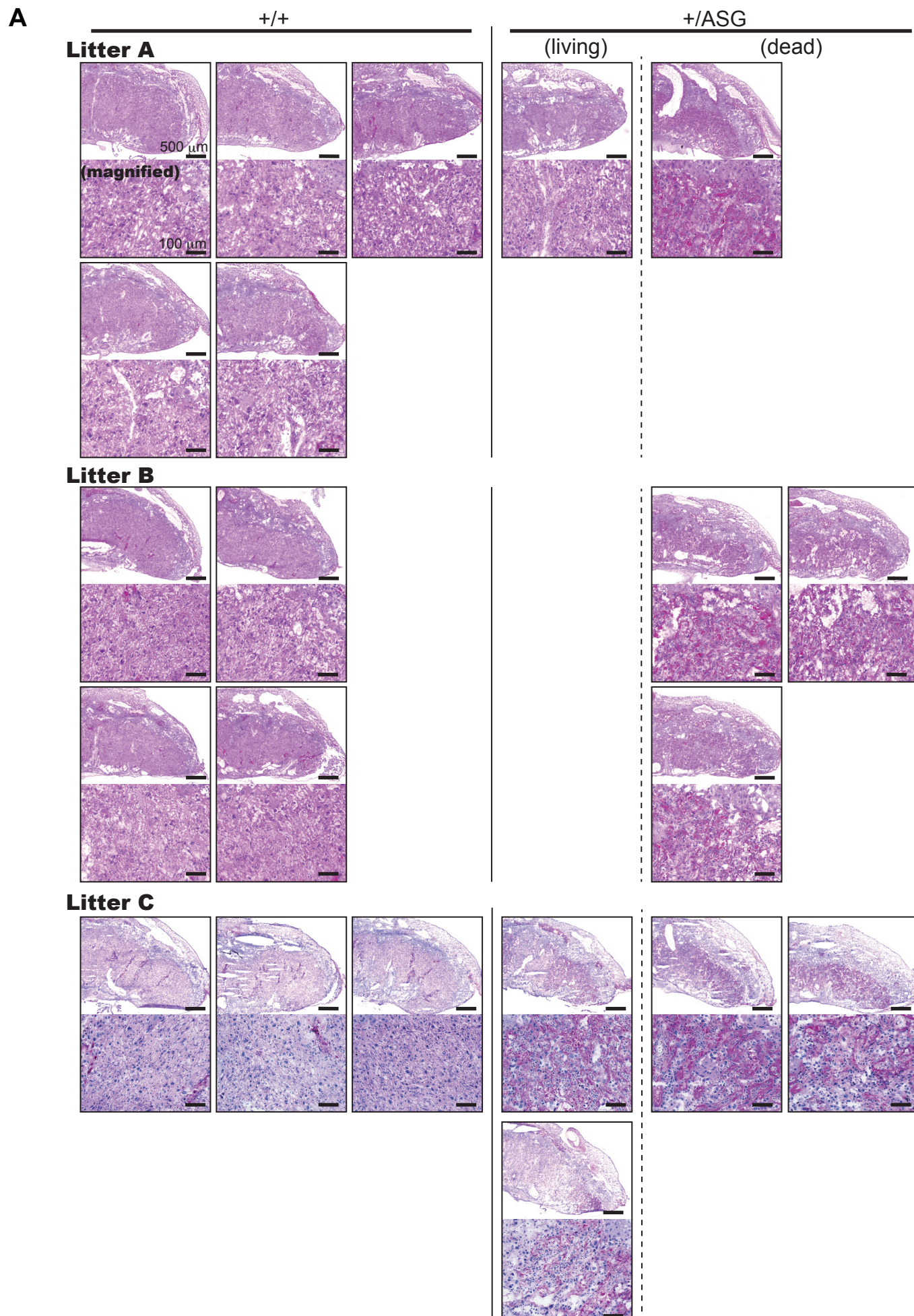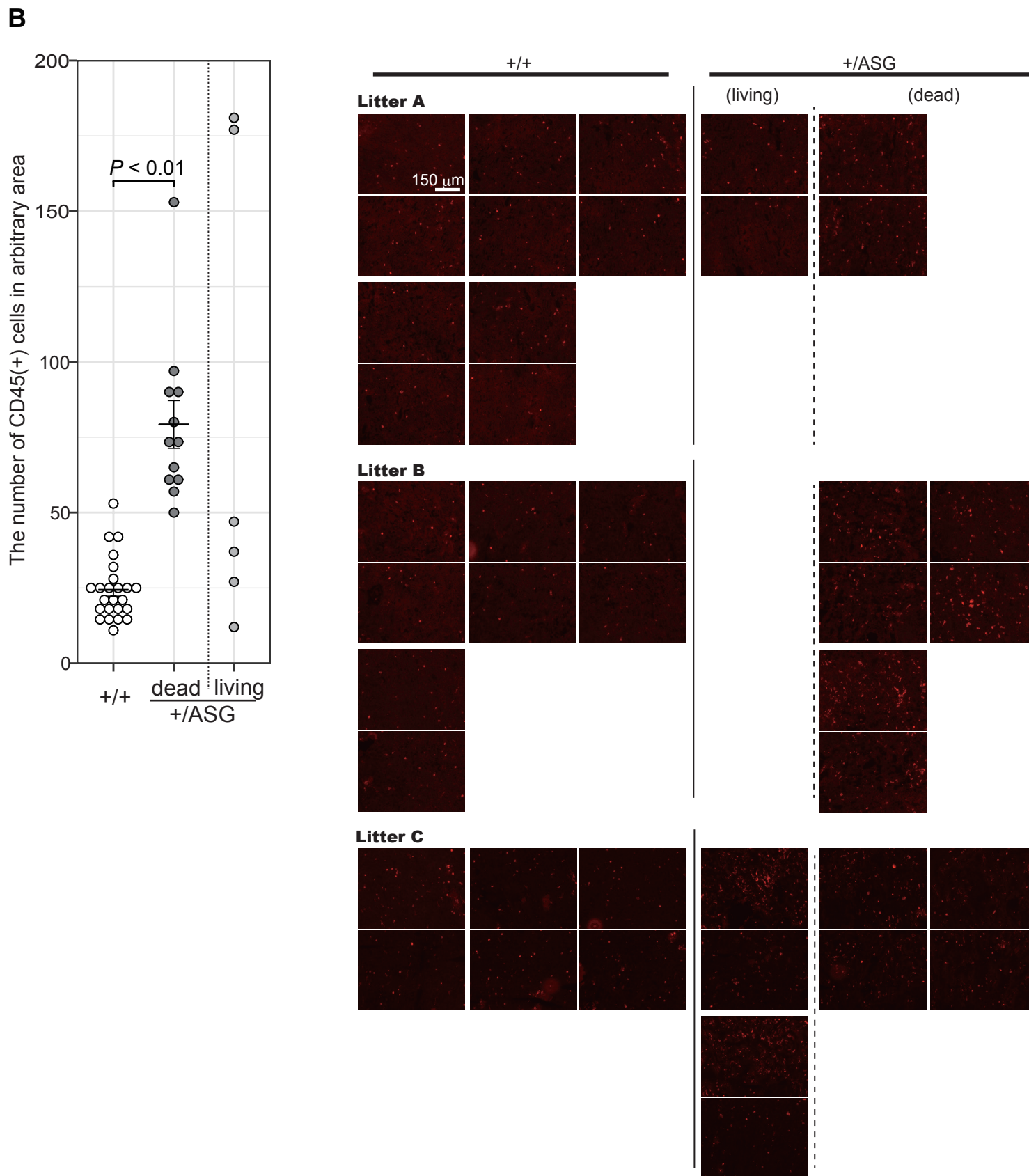
Fig. S7. Additional data related to Figures 3A and 3B.
(A) HE-stained histological sections of the 18.5 dpc placenta. (B) Comparison of the number of CD45-positive cells between +/+ and +/ASG in the 18.5 dpc placental labyrinth. Two CD45 immunofluorescence (IF) images were randomly acquired per placenta and the number of CD45-positive cells in each image was counted. The lines within the graphs indicate the mean value of each genotype and each dot represents the value acquired from each IF image. Statistical significance was calculated using a two-tailed unpaired Student's t-test with Welch's correction. The error bars indicate the s.e.m. All of the images analyzed are shown along with the plot.
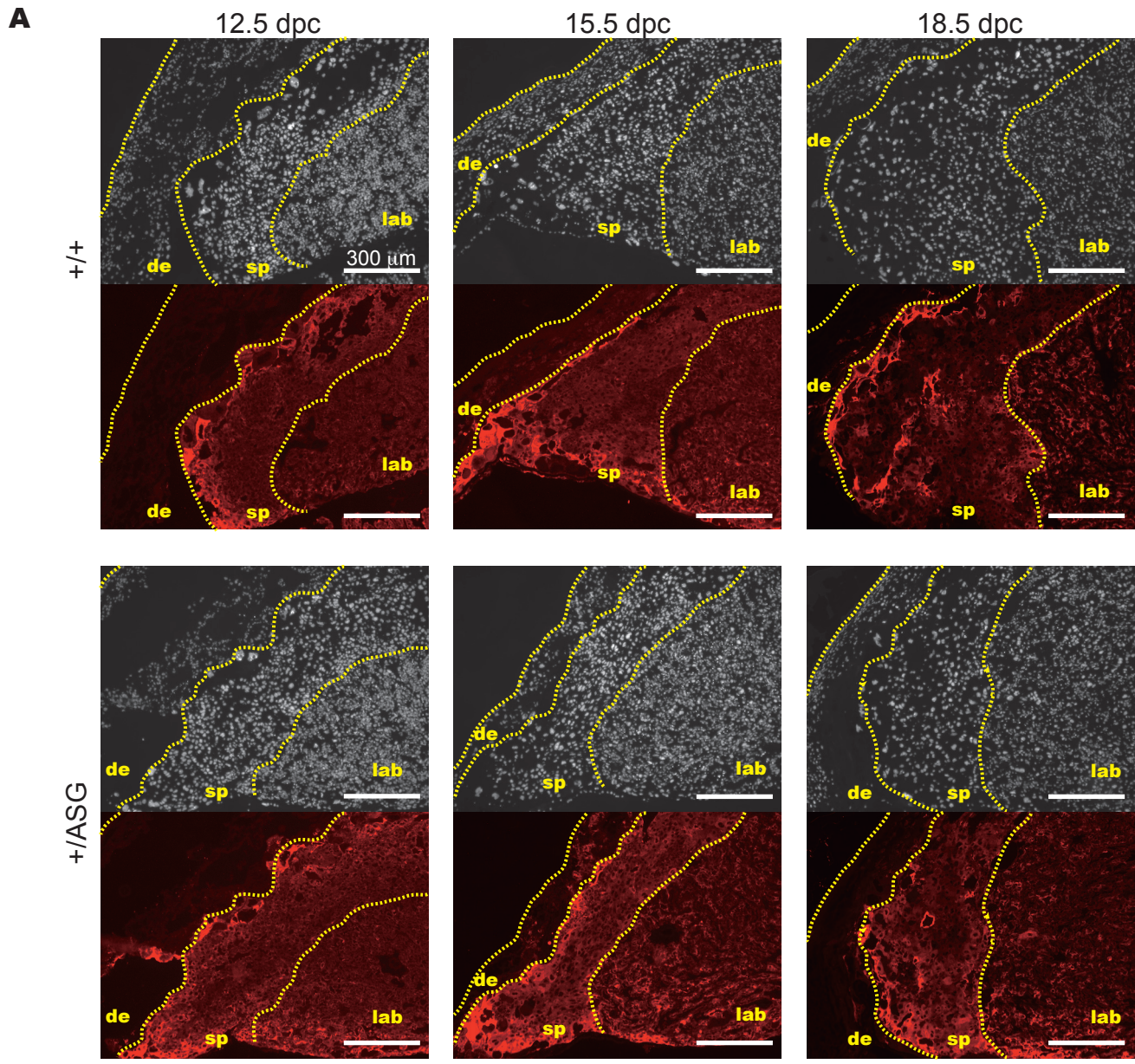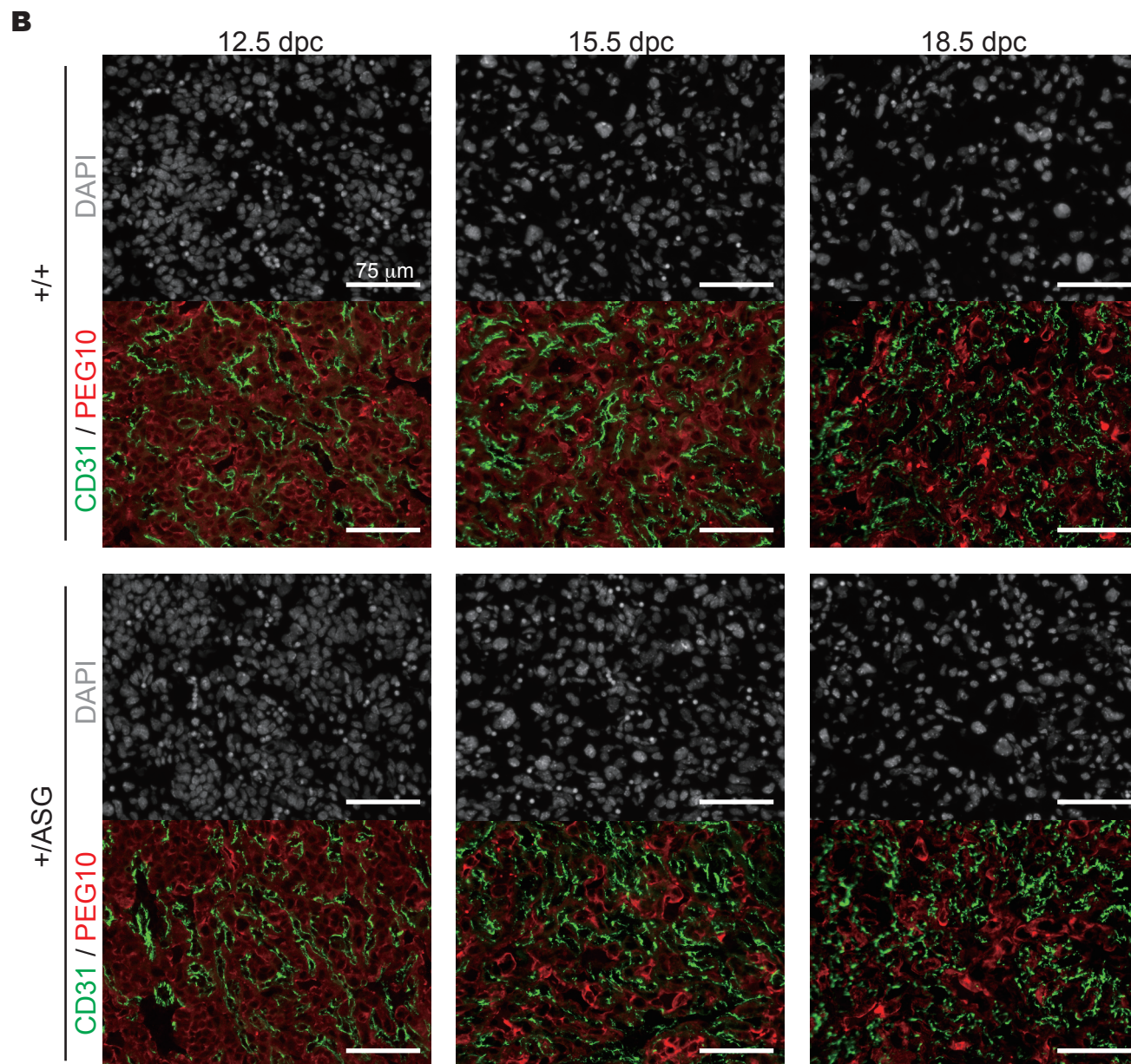
Fig. S8. PEG10 protein localization in placenta.

(A) PEG10 proteins (red) are distributed in all layers of the placenta except for the maternal decidua. The dotted lines indicate the edge of the maternal decidua, and the borders between the maternal decidua (de) and spongiotrophoblast (sp), and between the spongiotrophoblast (sp) and labyrinth (lab) layers. (B) Immunofluorescence analysis of the +/+ and +/ASG placenta with an anti-PEG10 (red) and CD31 (green) antibodies. Nuclei were stained with DAPI (white).
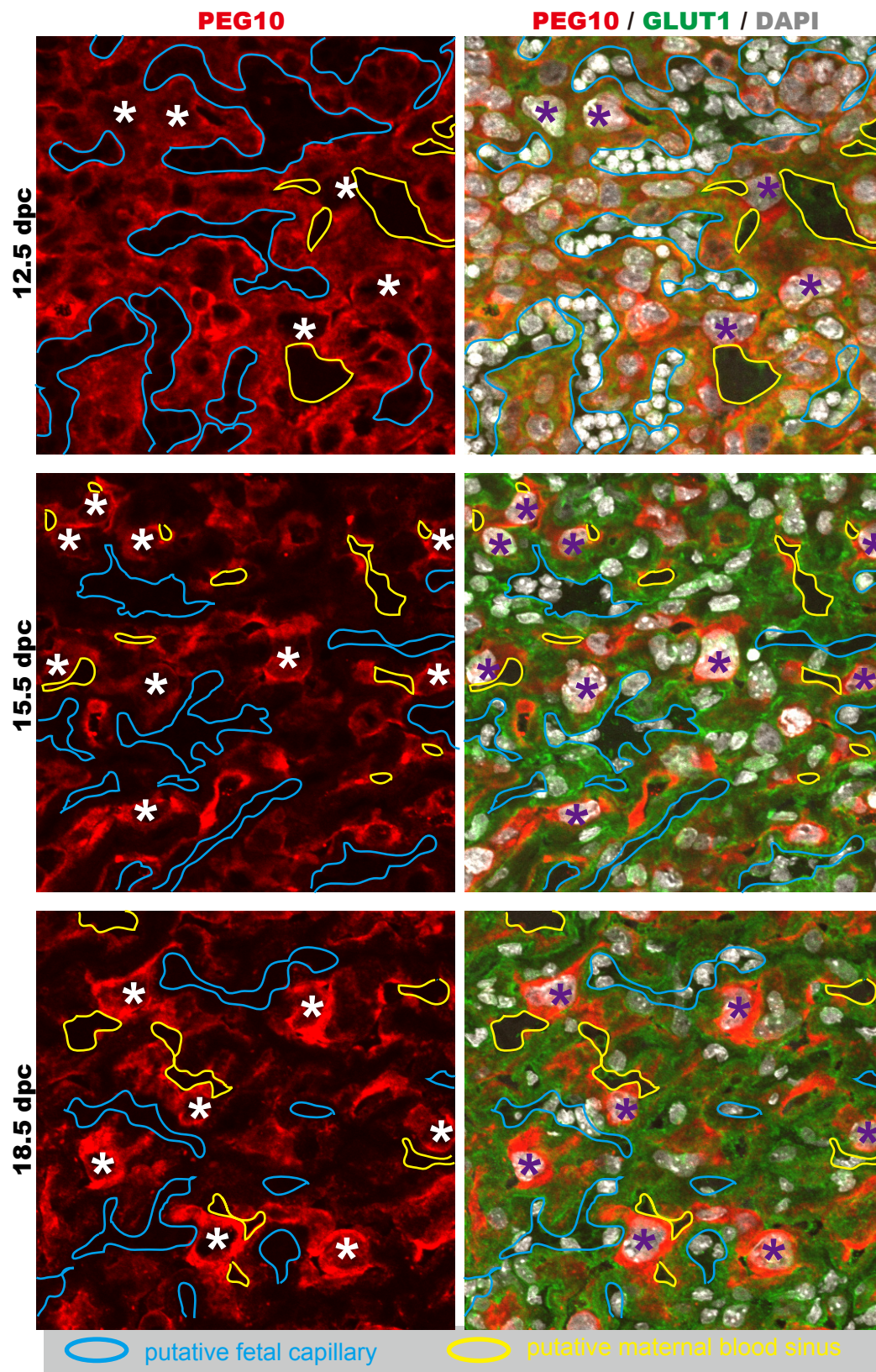
Fig. S9. Detailed analysis of PEG10 localization in placental labyrinth.

Immunofluorescence analysis of the wild-type placenta with anti-PEG10 (red) and GLUT1 (green) antibodies. Nuclei were stained with DAPI (white). GLUT1 is localized in the apical plasma membrane of the syncytiotrophoblast-I (SynT-I) facing the maternal blood sinus and basal plasma membrane of the SynT-II that faces the fetal blood capillaries. The putative fetal capillaries and maternal blood sinuses are enclosed by light blue and yellow lines, respectively. The asterisks indicate presumed s-TGCs nuclei.
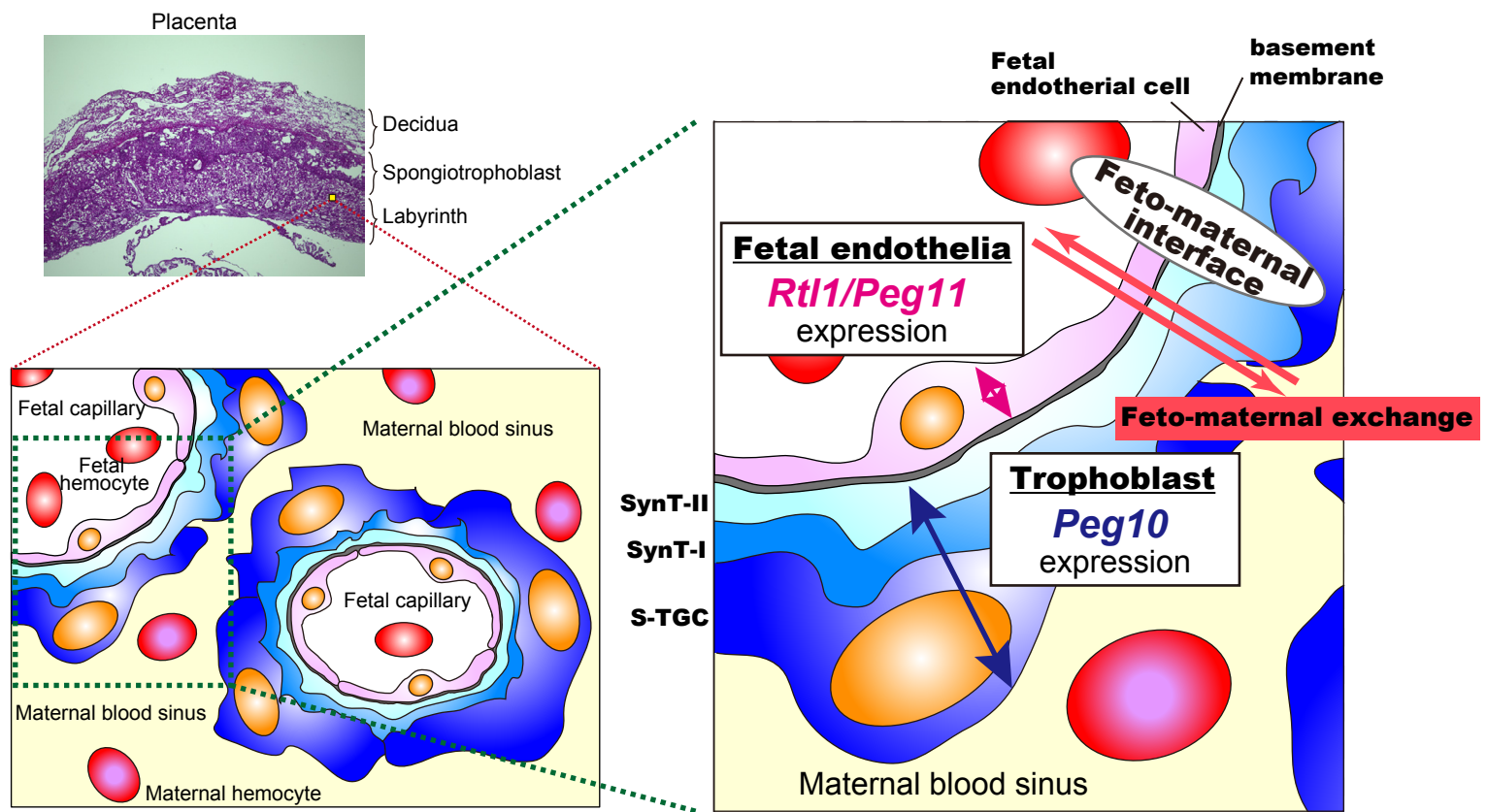
Fig. S10. A model for maintenance of fetal vascular network by *Peg10* and *Rtl1/Peg11*.
Two retrovirus-derived genes, *Peg10* and *Rtl1/Peg11*, function in trophoblast and fetal endothelial cells, respectively, acting at the feto-maternal interface to ensure normal feto-maternal exchange.